CONTRIBUTION OF GEAR BODY TO TOOTH DEFORMATION

Prof. M.Sc. Marunić G. PhD.
University of Rijeka Faculty of Engineering – Rijeka, Croatia

Abstract: *Through applying the 3D finite element method (FEM), the investigation into a spur thin-rimmed gear tooth deformation was performed. The developed geometrical and FEM models without manufacturing errors of the engaged solid pinion and thin-rimmed wheel, enabled the torque transmission and the tooth load distribution corresponding to actual wheel structure and its deformation as a whole.*
For the wheel body with thin rim supported by middle web, the chosen geometrical parameters of interest were the rim and web thickness, while the value of tooth face width was kept constant. A spur tooth deformations were determined and analysed through the deformation modus of the loaded tooth mid plane along the tooth height and along the face width, for the certain gear body flexibility.

Keywords: TOOTH DEFORMATION, THIN-RIMMED GEAR, GEAR BODY, FINITE ELEMENT ANALYSIS

1. Introduction

The relation between actual gear structure and gear tooth deformation represents an important issue in gear drive design considering the desirable weight gains and reduction of noise originated from the gearbox. In order to determine the best combination of gear body geometrical parameters it is important to evaluate their contribution to the gear teeth rigidity. Preliminary design orientations are needed to successfully connect different tools [1].

A powerful method for the determination of gear tooth state of stress and strain has become the finite element method (FEM) that has been usually compared with the results of previous investigations by means of analytical and experimental methods. Consequently, this method has supplied with additional insight into and has become the basis for important advances in gear design. This has been especially true for thin-rimmed gear teeth supported by complex body aggregated from a web that connects thin rim and hub. The gear body contributes to resultant gear tooth deformation and the load distribution along the tooth face width which has been considered by the development of various geometrical and numerical gear models. As thin-rimmed gear represents 3D structure more relevant investigation results have therefore been obtained by replacing 2D gear models with 3D ones. The 3D FEM gear models considerably differ on numerous aspects according to essential purpose they are built for.

A stress analysis of webbed gears has been mainly performed for the tooth root and adjacent area due to its importance for the estimation of gear strength [1, 2, 3].

An exhaustive 3D FEM analysis of thin-rimmed gear teeth stress and deflection can be found in [4, 5]. These investigations are characterized by the consideration of different structures of thin-rimmed gear (symmetric type single web gear, double web gear, thin-rimmed gears with and without ribs) and by the analysis of effects that the web, rib and rim thickness, and gear face width have mainly upon the stresses but on tooth deflection, too.

The problem of noise and vibration in the gear transmissions has been solved by use of dynamic models that evaluate the variations in mesh stiffness and transmission error [6, 7, 8].

As for the stress analysis of thin-rimmed gears, the modeling of gear deformation started with partial teeth models, until the advances in CAD systems have made possible to model whole gear deformations [9] and even entire gear transmission [10]. The issues of modeling proper load distribution over tooth face width, and the modeling of tooth contact zone have been solved differently by development of various methods [11, 12, 13].

The works worth to be mentioned regardless of different approaches to the gear modeling, but considering their generality and detailed elaboration of deformations and stresses arising at thin-rimmed webbed gears, are as follows [11, 9].

In [11] the subjects of investigation were the deformations and stresses at various locations at gear body with middle web. The attention was devoted to proper estimation of the load distribution along the tooth face width. Based on the known load distribution and the known reactions at the join of teeth and rim, the stresses and deformations at the rim and web were determined by means of the developed software using the FEM. The results represent valuable information gathered after consideration of numerous gear geometrical parameters such as gear diameter, tooth face width, rim and web thickness. Furthermore, it was found that the decreasing rigidity of gear body considerably diminishes the influence of contact lines errors upon the load unequal distribution along the tooth face width which results with greater efficiency of transmission.

Owing to the available powerful tool more recent work [9] than previously mentioned, analysed the deformations and stresses of thin-rimmed gear with offset web by applying whole gear deformation model. The load distribution was again calculated through the loaded tooth contact analysis by the 3D FEM and mathematical programming method. Then the loads were used to determine deformations and stresses by means of FEM. Among gear geometrical parameters were included the rim thickness, pressure angle and module, and their influence on tooth root, rim and web stresses were investigated. The analysis of stress achieved at the joint of thin rim and web pointed to the necessity to regard the joint as critical stress point additionally to the tooth root.

Furthermore, the rim circle deformation and web deformation were analysed. The comparison of transmission errors for a solid and thin-rimmed gear showed that vibration-exciting force of thin-rimmed gear is greater than for a solid gear. It was concluded too, that in the total deformations of thin-rimmed gear the rim and web

Fig.1. *3D FEM model (one half) of a solid pinion and thin-rimmed wheel engaged at the outer point of single pair tooth contact*; the points A, B, C *along the tooth height*

share about 70% and the gear teeth share only about 30%.

In this paper a solid pinion is mating with thin-rimmed wheel with middle web. Based on the experience and suggestions of previous investigations, the load distribution along the tooth face width resulting from actual gear structure is accomplished and whole wheel deformations are taken into consideration.

2. 3D Geometrical and FEM Model

The deformation of thin-rimmed spur gear mid-plane is determined for the pinion-wheel system of the following constant geometrical parameters: number of teeth $z_1=z_2=20$, modulus $m_n=10$ mm, pressure angle $\alpha_n=20°$, profile shift coefficient $x_1=x=0$, face width $b=100$ mm.

For the gear body with thin rim supported by middle web, the chosen geometrical parameters of interest were the rim and web thickness. The backup ratio s_R/h_t (s_R - rim thickness, mm, h_t – tooth height, mm) is chosen from 0,44; 0,64; 0,89 to 1,33.

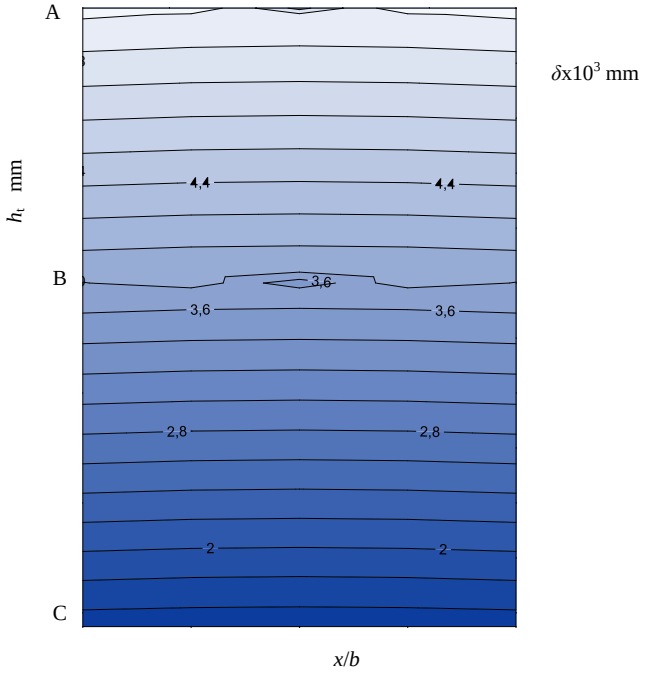

Fig. 2 *Contour plot of tooth displacement δ distribution along the tooth height and face width* (s_R/h_t=1,33; b_s/b=0,4)

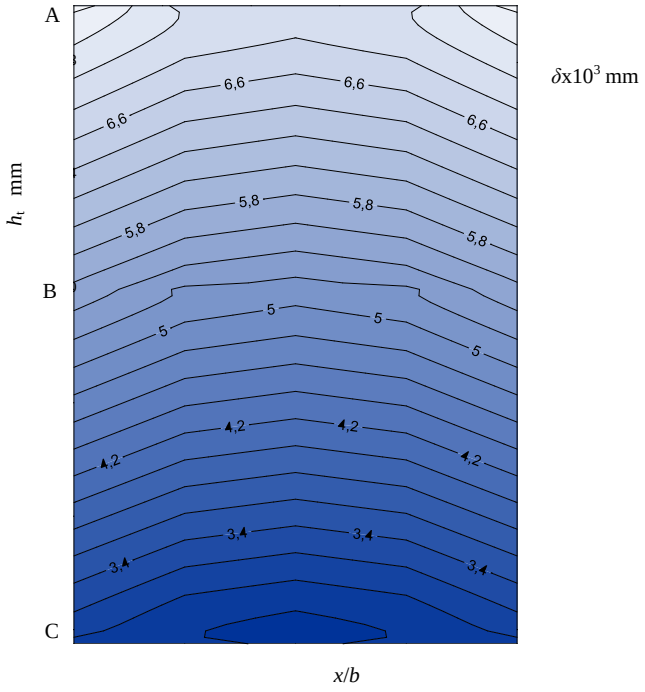

Fig. 3 *Contour plot of tooth displacement δ distribution along the tooth height and face width* (s_R/h_t=1,33; b_s/b=0,1)

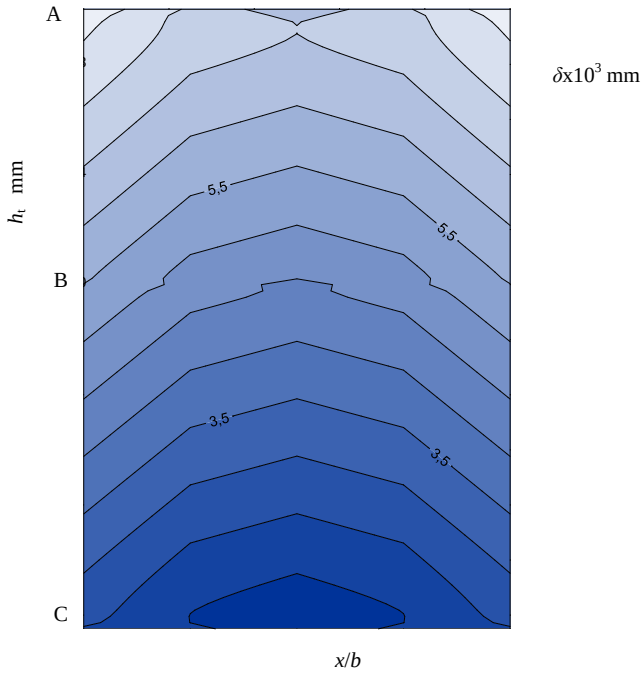

Fig. 4 *Contour plot of tooth displacement δ distribution along the tooth height and face width* (s_R/h_t=0,44; b_s/b=0,4)

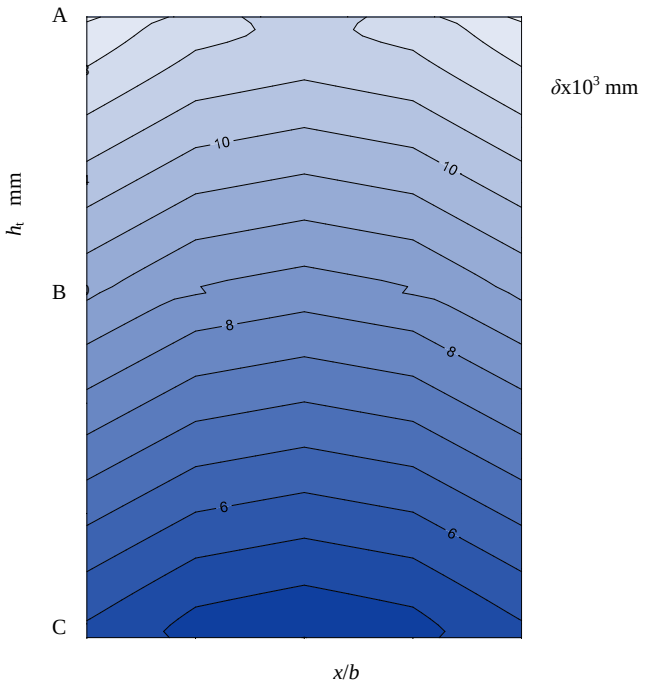

Fig. 5 *Contour plot of tooth displacement δ distribution along the tooth height and face width* (s_R/h_t=0,44; b_s/b=0,1)

These values overcome the backup ratio range proposed by the standard ISO [14] for thin-rimmed gear. The adopted web thickness is expressed by the ratio b_s/b (b_s – web thickness, mm): b_s/b =0,1; 0,2; 0,3 and 0,4.

The models of pinion and wheel differ as the pinion is partial gear model with three teeth and angular extension corresponding to four teeth, while the wheel is complete gear model with three teeth and other part of the rim made with increased rigidity that takes into account the excluded teeth (Fig. 1). The pinion and wheel are modeled in the outer point of single pair tooth contact. Due to the symmetry of geometry and load, the model with one half of the

actual face width is utilized.

The pinion-wheel system is subjected to constant torque and the imposed boundary conditions enable the simulation of torque transmission. The contact between the engaging teeth surfaces is accomplished by use of commercial software that detects frictionless contact. Due to non-linear contact problem and minute effect of Herzian local contact deformation on total tooth deformation, the tooth deformation is not followed at the point of contact but for the tooth mid-plane.

The tooth deformations were expressed by the magnitude of 3D displacements δ of tooth mid plane and were separated in the direction of tooth height and the tooth face width.

Fig. 1 shows the positions at the loaded tooth mid plane where the displacements are observed after the loading. The distribution of the displacements along the tooth height is followed for the points A (tooth tip), B (pitch point) and C (tooth root). Along the tooth face width five equally positioned points are chosen going from one to another tooth end.

3. Results and Discussion

The displacements were collected at the loaded tooth median surface. The distribution of displacements along the tooth height and face width is presented through the form of contour plot in Fig. 2, 3, 4, 5. Among the obtained results there were separated the combinations of rim and web thickness that represent extreme conditions of gear body flexibility. The direction of the tooth face width b is expressed by no dimensional coordinate x/b.

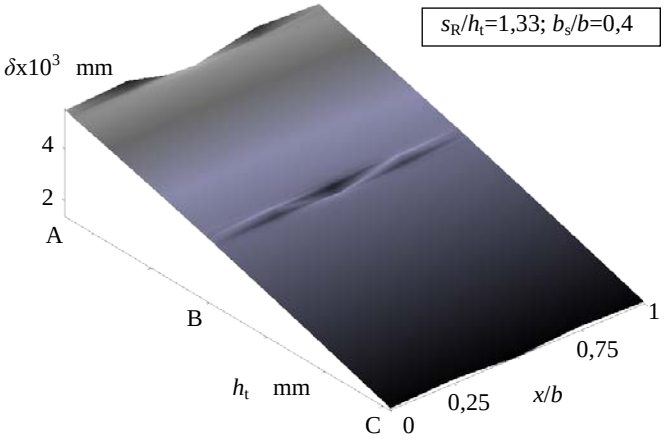

Fig. 6 *The loaded tooth displacements δ along the tooth height and face width* (s_R/h_t=1,33; b_s/b=0,4)

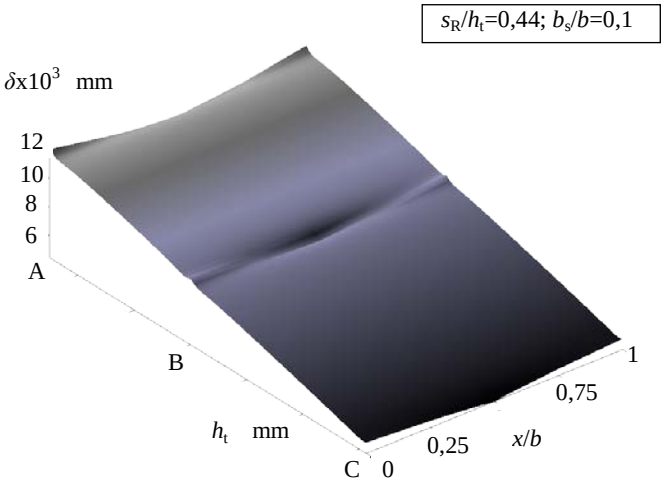

Fig. 7 *The loaded tooth displacements δ along the tooth height and face width* (s_R/h_t=0,44; b_s/b=0,1)

3.1. The distribution of tooth displacements along the tooth height

Maximum displacements are always reached at the tooth tip and their magnitude considerably depends on the certain combination of rim and web thickness. In comparison with the combination of the greatest value of rim and web thickness under consideration (s_R/h_t=1,33; b_s/b=0,4), the diminishing of web thickness to minimum value (b_s/b=0,1) increases maximum displacements (reached at the face width) going from the tooth root C towards the tip A, for 85% and 34%, respectively (Fig. 2, 3).

As regards the thinnest rim supported by the thickest web (s_R/h_t=0,44; b_s/b=0,4) and going towards the thinnest web (b_s/b=0,1), the increment of maximum displacements is much more obvious and overcomes the initial values for twice and 54% when moving from the tooth root C towards the tip A (Fig. 4, 5).

The actual flexibility change of gear body affects mostly the variation of displacement δ at the tooth root and this influence diminishes going towards the tooth tip. The displacements for thin rim (s_R/h_t=0,44) generally increase more along the tooth height with the decrease of web thickness and for the combination of the thinnest rim and web severe displacement increment at the tooth root is evident.

In Fig. 6,7 the tooth displacements δ are shown along the tooth height and face width in the form of surface plot, for the gear body with the thickest rim and web (s_R/h_t=1,33; b_s/b=0,4) and with the thinnest rim and web (s_R/h_t=0,44; b_s/b=0,1). The variation of the displacements along the tooth height is evident for both combinations of rim and web thickness applied for the gear body, but the displacement for the thickest rim and web going from the tooth root C towards the tip A increases more.

Fig. 8 presents maximum displacement δ_{max} at the tooth tip regardless of the position along the tooth face width, achieved

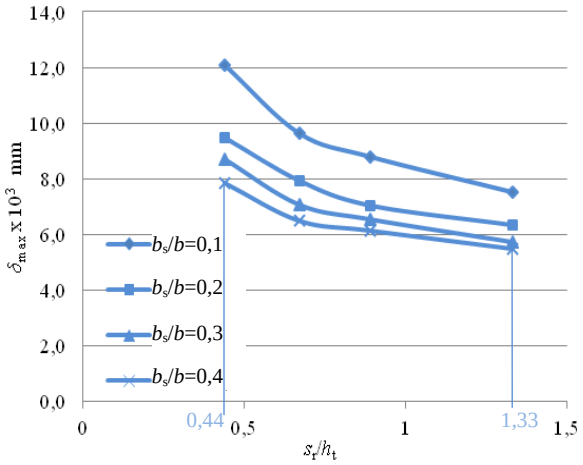

Fig. 8 *The relationship between maximum tooth displacement δ_{max} and rim and web thickness*

for different web thickness and related to the rim thickness. As the web thickness increases from b_s/b=0,1 to 0,4, maximum tooth displacements diminish depending on the rim thickness, for 35% (s_R/h_t=0,44) and for 27% (s_R/h_t=1,33). The increment of rim thickness from s_R/h_t=0,44 to 1,33, results with the decrease of maximum displacements for 38% (b_s/b=0,1) and for 30% (b_s/b=0,4).

3.2. The distribution of tooth displacements along the tooth face width

The displacement distribution that is followed along the face width for equally positioned points, shows significant differences in relation to the influence of both, the rim and web thickness. At the position of middle web the tooth deforms less in comparison to the tooth edges (Fig. 6, 7).

Fig. 9 presents the ratio δ_e/δ_m of displacement δ_e at the tooth

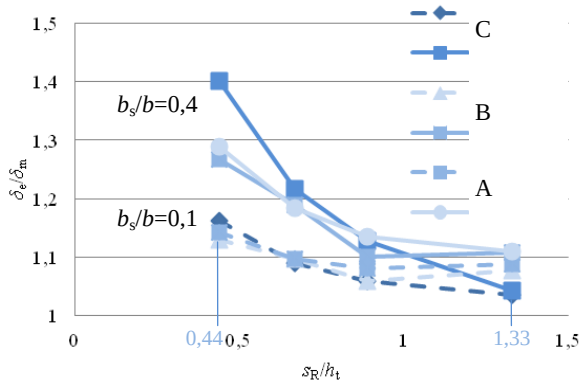

Fig. 9 *The ratio* δ_e/δ_m of displacements *along the tooth height for the thinnest* (b_s/b=0,1) *and thickest* (b_s/b=0,4) *web, related to the rim thickness* s_R/h_t *(displacement* δ_e *at the tooth edge and displacement* δ_m *at the middle of the tooth face)*

edge and the displacement δ_m in the middle of the tooth face, for the points A, B, C along the tooth height and related to the rim thickness s_R/h_t. For the sake of clarity, there are included the thinnest and thickest web.

Non uniform displacement distribution along the tooth face width varies along the tooth height: for the thickest rim non uniformity diminishes going from the tooth tip A towards the root C, and for the thinnest rim the tooth root C distribution shows the greatest non uniformity. As the rim thickness diminishes displacement distribution becomes more non uniform, but much more for the thickest web (b_s/b=0,4). Non uniformity of displacements along the tooth face width is maximum for the thinnest rim supported by the thickest web (s_R/h_t=0,44; b_s/b=0,4), and at the tooth root C the displacement at the tooth edge is about 40% greater than the corresponding one in the middle of face width (Fig. 4, 9).

For the thinnest rim and web (s_R/h_t=0,44; b_s/b=0,1) when the displacements take maximum values, non uniformity of distribution along the tooth face for certain tooth height, differs slightly (Fig. 7, 9).

4. Conclusions

The results about the loaded tooth deformation obtained at the tooth mid plane after loading, confirmed considerable impact of the actual combination of rim and web thickness of a spur gear with middle web.

Maximum displacements are always reached at the tooth tip. By the decrease of web thickness the displacements increase going from the tooth root towards the tooth tip, but more for the thinnest rim. The actual flexibility change of gear body affects mostly the variation of displacements at the tooth root and going towards the tooth tip this influence diminishes. For the combination of the thinnest rim and web a severe increment of tooth root displacements occurs.

As for the displacement distribution along the tooth height, the impact of rim and web thickness can be noticed through non uniform displacement distribution along the tooth face width, too.

In relation to the tooth height, non uniform displacement distribution along the face width for the thinnest rim supported by the thickest web is mostly expressed, while for the thickest rim non uniformity of distribution is less obvious, regardless of the web thickness.

For the thinnest rim and web when the displacements take maximum values, non uniformity of distribution along the tooth face for certain tooth height, differs slightly.

5. Literature

[1] Kim, H. C., Vaujany, J. P., Guingand, M., Play, D. Stress Analysis of Cylindrical Webbed Spur Gears: Parametric Study - Journal of Mechanical Design, Vol. 180, 1998, pp 349 - 357.

[2] Blazakis, A., Houser, D. R., in: Proceedings of the International Gearing Conference, 1994, pp 149-154.

[3] Baret, C., Coccolo, G., Raffa, F.A., in: Proceedings of International Gearing Conference, 1994, pp. 149-154,

[4] Sayama, T., Oda, S. Study of Welded Structure Gears - Bulletin of JSME, Vol. 27, No. 230, 1984, pp. 1773-1779.

[5] Sayama, T., Oda, S., Umezawa, K. Study of Welded Structure Gears - Bulletin of JSME, Vol. 29 No. 256, 1986, pp. 3582-3586.

[6] Wadkar, S. B., Kajale, S. R., in: Proceedings of the 14th ISME International Conference on Mechanical Engineering in Knowledge Age, December 12-14, 2005, pp 148-153.

[7] Wadkar, S. B., Kajale, S. R., Gupta, K., Desai, G. M., in: Proceedings of International Conference on Advances in Machine Design & Industry Automation, January 10-12, 2007, pp 89-93.

[8] Rigaud, E., Barday, D., in: Proceedings of 4th World Congress on Gearing and Power Transmissions, March 16-18, 1999, pp 1961-1970.

[9] Li, S. Deformation and Bending Stress Analysis of Thin - Rimmed Gear - Journal of Mechanical Design, Vol. 124, 2002, pp 129-135.

[10] Tian Yong, T., Li Cong, X., Tong, W., Wu Chang, H. A Finite–Element–Based Study of the Load Distribution of a Heavily Loaded Spur Gear System with Effects of Transmission Shafts and Gear Blanks – Journal of Mechanical Design, Vol. 125, 2003, pp 625-631.

[11] Linke, H., Mitsche, W. Senf, M. Einflußder radkorpergestaltung auf die tragfähigkei von stirnradverzahnungen - Maschinenbautechnik, Vol. 32, No 10, 1983, pp 450-457.

[12] Prabhu, M. S., Houser, D. D. R. in : Proceedings of International Conference of Gears, 1996, pp 201-212.

[13] Li, S. Gear Contact Model and Loaded Toot Contact Analysis of a Three - Dimensional, Thin-Rimmed Gear - Journal of Mechanical Design, Vol. 124, 2002, pp 511-517.

[14] ISO 6336 - 3 Calculation of load capacity of spur and helical gears - Part 3: Calculation of tooth bending strength, 2006.